THE ASTROPHYSICAL JOURNAL, 213:18–26, 1977 April 1

PLANETARY NEBULAE IN LOCAL GROUP GALAXIES. IV. IDENTIFICATIONS, POSITIONS, AND RADIAL VELOCITIES OF NEBULAE IN NGC 147 AND NGC 185

HOLLAND C. FORD, GEORGE JACOBY, AND DAVID C. JENNER
Department of Astronomy, University of California, Los Angeles
Received 1976 July 6; revised 1976 September 9

ABSTRACT

We present identifications of five planetary nebulae in NGC 147. Equatorial coordinates are presented for the nebulae and reference stars in NGC 147 and for five nebulae and reference stars in NGC 185. The coordinates have an accuracy better than 1″.0 relative to the AGK3 and better than 0″.5 relative to one another. The radial velocity of NGC 185 (-208 km s^{-1}) has been determined from observations of two of its planetary nebulae. The first radial velocity for NGC 147 (-168 km s^{-1}) has been determined from observations of its brightest planetary nebula. Consideration of the radial velocities leads us to conclude that the two galaxies do not form a gravitationally bound system. The five planetary nebulae identified in each galaxy provide a direct observational basis for estimating the rate at which mass returns to the interstellar media in the galaxies. We estimate that the hydrogen mass loss rate is $\dot{M} \geqslant 8 \times 10^{-5}\ M_\odot\ \mathrm{yr}^{-1}$. On the basis of our estimates of the mass and stellar velocity dispersion in NGC 147, we conclude that the expanding planetary shells can power a thermally steady galactic wind in NGC 147. There is a strong likelihood that supernova heating of the cool interstellar medium results in a hot wind blowing from NGC 147.

Identifications and equatorial coordinates for globular clusters in NGC 147(4) and NGC 185(6) are presented in the Appendix.

Subject headings: clusters: globular — galaxies: clusters of — galaxies: individual — galaxies: stellar content — nebulae: planetary — stars: mass loss

I. INTRODUCTION

The isolation and observation of planetary nebulae in elliptical galaxies allow direct determination of important properties such as chemical abundances, stellar velocity dispersion, and the rate of production of an interstellar medium. Ford, Jenner, and Epps (1973, hereafter Paper I) presented identifications of planetary nebulae in NGC 185 (4), NGC 205 (12), and NGC 221 (10). Ford and Jenner (1975, hereafter Paper II) extended the identifications in NGC 221 (M32), estimated the total number of nebulae in that galaxy, and estimated the rate at which mass is returned to the interstellar medium by planetary nebulae. Ford and Jenner (1976, hereafter Paper III) presented radial velocities for two of the faint diffuse nebulae in the M32 field and concluded that the two nebulae are H II regions in the M31 spiral arm which projects across the M32 field.

In this paper we present the first identifications of planetary nebulae in NGC 147(5). The equatorial coordinates of the planetary nebulae and nearby reference stars in NGC 147 and NGC 185 are presented in § II. Radial velocities of nebulae in NGC 147 and NGC 185 are presented in § III. In § IV we discuss the gravitational binding of NGC 147 and NGC 185, the production rate of their interstellar media, and the possibility that a galactic wind is blowing in these galaxies.

In the course of this work we searched all available Lick Observatory 120 inch (3.05 m) telescope plates of NGC 147 and NGC 185 for globular clusters. The identifications and equatorial coordinates of the clusters and nearby reference stars are presented in the Appendix.

II. IDENTIFICATIONS AND POSITIONS

a) NGC 147

Our identification technique, which is based on pairs of on-line and off-line interference filter photographs, is discussed in Paper I. In that paper the authors were unable to identify any planetary nebulae in NGC 147 with a pair of exposures made during poor seeing through filters whose central wavelengths (λ_c) and full widths at half-maximum (FWHM) were λ_c5020 (57 Å FWHM) and λ_c5300 (200 Å FWHM). The following year NGC 147 was photographed during good seeing ($\sim 1\frac{1}{2}''$) with a pair of interference filters whose characteristics are λ_c6565 (21 Å FWHM) and λ_c6065 (175 Å FWHM). This very effective isolation of Hα enabled us to identify five faint planetary nebulae in NGC 147.

Figure 1 (Plate 1) is a reproduction of a 30-minute exposure with the λ_c6565 (21 Å FWHM) filter and a Westinghouse WL-30677 image intensifier plus a IIa-D photographic plate. The planetary nebulae are identified with arabic numerals.

TABLE 1

IDENTIFICATIONS OF PLANETARY NEBULAE IN NGC 147 AND NGC 185

NGC 147		NGC 185	
ED 2590 1972 Aug. 13–14 20 minutes IIa-D 5020/57	ED 2670 1973 Aug. 27–28 30 minutes IIa-D 6565/21	ED 2575 1972 Aug. 12–13 30 minutes IIa-D 5020/57	ED 2586 1972 Aug. 13–14 30 minutes IIa-D 5020/57
...	1*	1*	1*
...	2	2*	2*
...	3	3	3
...	4	4	4
...	5	5	5

* A radial velocity has been measured.

TABLE 2

COORDINATES OF PLANETARY NEBULAE AND REFERENCE STARS IN NGC 147

Designation	Right Ascension (1975.0)	Declination (1975.0)
	Planetary Nebulae	
1...........	$00^h31^m50^s.37$	48°20′02″.0
2...........	00 32 02.86	48 21 29.7
3...........	00 32 06.43	48 24 51.8
4...........	00 31 49.57	48 24 01.9
5...........	00 31 51.17	48 20 50.1
	Reference Stars	
a...........	00 31 44.25	48 20 15.6
b...........	00 31 47.18	48 24 08.9
c...........	00 31 48.34	48 22 17.6
d...........	00 31 50.56	48 20 34.0
e...........	00 31 52.80	48 18 26.1
f...........	00 32 01.79	48 21 39.0

A summary of the NGC 147 plate material and identifications is included in Table 1. Each column is headed by the plate number, date of the photograph, exposure time, plate type, and characteristics of the filter. The presence of an arabic numeral in the column indicates that the corresponding nebula was identified on that plate.

Spectrophotometry of planetary nebulae as faint as these typically requires precise blind offsets. Equatorial coordinates of the nebulae and nearby reference stars are presented in order to facilitate such difficult observations. In Paper II it was shown that our WL 30677 image intensifier is especially suitable for this work, since it has no geometrical distortion on a scale larger than 0″.5 (25 micrometers on the anode).

Paper II described our technique of using Lick Observatory 20 inch (51 cm) Carnegie astrograph plates as an intermediate step in the transformation of the positions of the planetary nebulae and reference stars to the AGK3 system. A least-squares fit of the positions of 39 AGK3 stars on the astrograph plate AY 6345 to their standard coordinates, equinox 1975.0, using the polynomial which is appropriate for Eichhorn's (1974) "standard model" resulted in a standard deviation of 0″.34 in each coordinate. A linear least-squares transformation of 14 reference stars on the image-intensifier plate ED 2670 to their standard coordinates, equinox 1975.0, gave standard deviations of 0″.44 in right ascension and 0″.32 in declination.

The equatorial coordinates of the five planetary nebulae and six of the reference stars are presented in Table 2. The first column gives the designations of the nebulae (arabic numerals) and reference stars (roman letters), as marked in Figure 1. Column (2) gives the right ascension, and column (3) gives the declination, both for the equinox of 1975.0.

The precision of the coordinates, which is discussed in § II*b*, is estimated to be at least 1″.0 relative to the AGK3 and at least 0″.5 relative to one another.

b) *NGC 185*

In Paper I two pairs of λ5007 on-line and off-line plates were used to identify four planetary nebulae in NGC 185. Subsequently, these plates were used to identify an additional faint nebula near the center of the galaxy. Since the nebula can be detected against the bright envelope of the galaxy, it may be the most luminous planetary nebula in NGC 185. The plate material and identifications are summarized in Table 1.

The transformations of the image-intensifier plates ED 2575 and ED 2586 (cf. Table 1) to the AGK3 were made through 14 AGK3 stars on the astrograph plate AY 8063 kindly taken for us by Dr. Arnold Klemola. The standard deviation of the transformed astrograph measurements was 0″.20 in each coordinate. The average standard deviations resulting from the linear transformations of 20 reference stars on the two image-intensifier plates to standard coordinates were 0″.3 in each coordinate. The small residuals indicate a high degree of internal consistency. A better measure of internal consistency is given by comparing the positions of the planetary nebulae derived from the two image-intensifier plates. The average standard deviation about the mean positions is 0″.14 in right ascension and 0″.26 in declination. The much larger body of data in Paper II allowed us to conclude that those coordinates had an external accuracy relative to the AGK3 of at least 1″.0 and a differential accuracy of at least 0″.5. The present data indicate that these coordinates have the same precision as those in Paper II.

The equatorial coordinates of the five planetary nebulae and seven reference stars are presented in Table 3. The column headings have the same meanings as in Table 2. The coordinates of the planetary nebulae and stars, except d and g, are the averages from the linear transformations of the two image-intensifier plates. The coordinates of star g are its AGK3 coordinates; those of d are determined from only one plate.

An identification photograph for the first four planetary nebulae is given in Paper I. Figure 2 (Plate 2) is a reproduction of the central portion of a photograph of NGC 185 taken by Dr. N. U. Mayall on 1960 August 26–27. The 40-minute exposure (ED 354)

TABLE 3

COORDINATES OF PLANETARY NEBULAE AND REFERENCE STARS IN NGC 185

Designation	Right Ascension (1975.0)	Declination (1975.0)
	Planetary Nebulae	
1..........	00h37m33s62	48°11′08″0
2..........	00 37 30.02	48 11 54.3
3..........	00 37 37.10	48 11 33.9
4..........	00 37 24.90	48 11 18.1
5..........	00 37 34.17	48 11 56.7
	Reference Stars	
a..........	00 37 21.27	48 11 44.1
b..........	00 37 29.70	48 12 28.5
c..........	00 37 31.83	48 11 09.6
d..........	00 37 36.76	48 11 52.7
e..........	00 37 45.51	48 15 08.2
f..........	00 37 51.31	48 11 23.7
g*........	00 38 13.285	48 19 36.03

* Star g = AGK3 48°00660; the coordinates are AGK3, equinox and epoch 1975.0.

was made with a 103a-E plate and Schott GG 11 filter at the prime focus (B Ross corrector) of the 120 inch telescope. This plate resolves NGC 185 into stars. It is presented here for the identifications of the globular clusters which are discussed in the Appendix. The reference stars in Table 3 are marked in Figure 2 with roman letters.

III. RADIAL VELOCITIES OF THE PLANETARY NEBULAE

Accurate radial velocities of planetary nebulae in Local Group galaxies allow us to establish their membership in a particular galaxy (e.g., planetary nebulae in M32, Paper II), investigate the galaxy's internal dynamics, and, in a galaxy like NGC 147, which has no previously measured radial velocity, determine its dynamical relationship to another galaxy such as NGC 185. In subsequent papers we will discuss the radial velocities of planetary nebulae in M32, in NGC 205, and in selected fields in M31. Here we give a detailed description of observational and reduction techniques.

a) *Observations*

The observations were made with the image-tube scanner (ITS) developed by Robinson and Wampler (Robinson and Wampler 1972*a*, *b*) mounted on the Lick Observatory Cassegrain spectrograph (Miller, Robinson, and Wampler 1975). The Cassegrain spectrograph allows very convenient and flexible observing, since *all* spectrograph functions can be controlled remotely from the 120 inch telescope control room.

For observations at Hα, a 1200 line mm^{-1} grating is used in the first order ($\lambda_{\rm blaze}$ = 5000 Å). The reciprocal dispersion at the image dissector, which has a 20 μm entrance slot, is approximately 78 Å mm^{-1}, or 0.63 Å per channel when the 20 mm of spectrum is digitized into 2048 channels. A neon lamp is the comparison source.

For observations of Hβ, λ4959, and λ5007, a 830 line mm^{-1} grating is used in the second order ($\lambda_{\rm blaze}$ = 8465 Å). The reciprocal dispersion at the image dissector is approximately 56 Å mm^{-1}, or 0.48 Å per channel. A helium-mercury lamp is the comparison source.

Except for very low-excitation nebulae, the higher-dispersion observations with the 830 line mm^{-1} grating are more efficient than those with the 1200 line mm^{-1} grating. There are three reasons for this: (1) the extended S-20 photocathode of the first image intensifier has peak sensitivity in the blue-green; (2) the sky is darker in the blue-green than in any other visible spectral region (Broadfoot and Kendall 1968; Arp 1964); and (3) moderate- to high-excitation nebulae have better contrast in the blue-green than in the red when seen against the envelope of the parent galaxy.

The nebulae are acquired by using the 120 inch telescope intensified secondary emission conduction (ISEC) television system and a movable reticle with a digitized *x-y* stage to blind-offset from the reference stars. Because of flexure in the *x-y* stage and the fact that the nebulae are too faint to be seen, it is not sufficient to simply blind-offset to the nebula's position. Acquisition requires the combination of a raster search with varying the size of entrance aperture. The accumulating memory of the scanner system is displayed on a CRT, supplying a real-time indication of the signal rate. This provides us with a means to acquire and center the nebula, usually within 30 minutes. The observations are made with a 2″ × 2″ entrance aperture.

Our choice of integration sequences is determined by the signal from the planetary nebula relative to the "noise" of the underlying galaxian stellar continuum. If the stellar continuum is relatively strong, it is necessary to subtract it out; otherwise the underlying absorption line may change the apparent positions of the emission lines. In such cases we typically use the following sequence of 4-minute integrations: object, sky, object . . ., where the sky observations are taken 5″ from the object at the cardinal points. In those cases where the underlying stellar continuum is weak or effectively absent (halo objects), a maximum signal-to-noise ratio is obtained by spending all the integration time on the object.

There are three possible sources of systematic velocity errors in the ITS–spectrograph combination. The first is a slow drift in the electronic registration of successive scans of the last image-tube phosphor by the image dissector. The second is flexure in the ITS–spectrograph; the third is a difference between the illumination of the collimator by a star and its illumination by the comparison source. In § III*c* we will show that the last is not a problem.

Our data show that flexure is much more of a problem than electronic instabilities. Flexure can result in shifts of the spectrum by as much as 4 channels from one position in the sky to another. We minimize the effects of both error sources by taking a spectrum of the comparison source immediately before and one immediately after the sequence of observations of the object. The mean difference in registration between the before and after spectra determined from observations of 16 extragalactic planetary nebulae is 0.04 channels; the standard deviation from the mean is 0.30 channels. These values show that flexure errors can be eliminated.

The two semistellar planetary nebulae VY2–3 and M1–2 (Perek and Kohoutek 1967) were observed as radial-velocity standards. The choice of semistellar nebulae eliminates spatial-velocity variations as an error source. A 2.5 mag gelatin neutral density filter is used behind the slit to reduce the persistence in the last phosphor of the ITS that results from observing bright nebulae.The radial velocities of these nebulae will be discussed in § III*c*.

b) *Radial-Velocity Reductions*

Line positions in the nebulae are determined by using a PDP11 computer to sum the 4-minute integrations into a single nebula-plus-sky or nebula spectrum. The spectrum is displayed on a Tektronix 4010 graphics display terminal, where a cursor is used to delimit and expand emission-line segments of the spectrum. The emission lines are then visually bisected with the cursor. This procedure determines line positions to an accuracy of approximately $\frac{1}{3}$ channel.

The preceding and following comparison scans are added together before being measured. Wavelengths are determined from a least-squares cubic polynomial fit of the comparison spectrum. The rms residuals of the neon spectra are typically 0.3 Å, which is comparable to the measuring errors. When working in the blue-green spectral region, the grating is set at the maximum allowable tilt in order to position λ5007 as far as possible from the edge of the spectrum. Though only four helium lines (λ4471, 4713, 4921, and 5015) can be used to determine the dispersion at this setting, the lines Hβ, λ4959, and λ5007 are so close to comparison lines that the resultant radial velocities have high precision.

c) *Radial-Velocity Error Analysis*

The ITS radial velocities of the galactic planetary nebulae VY2–3 and M1–2 are presented in Table 4. The emission lines and spectrograph slits are treated individually, since there may be wavelength and slit-dependent errors. The first column in Table 4 gives the planetary nebula's designation. Column (2) gives the slit used for the observation; column (3) gives the wavelength of the emission line; column (4) gives the average heliocentric radial velocity for the planetary nebula determined by the emission line; column (5) gives the standard deviation from the mean; and column (6) gives the number of independent observations of the line. All observations were made during the 1975 observing season except those marked with an asterisk (1974 observing season). The rest wavelengths used for the nebular lines are λ4958.92 and λ5006.85 (Bowen 1960), and for the hydrogen lines λ4861.33 and λ6562.81.

TABLE 4

RADIAL-VELOCITY OBSERVATIONS OF TWO SEMISTELLAR GALACTIC PLANETARY NEBULAE

Planetary Nebula (1)	Slit (2)	Line (3)	v_0 (km s^{-1}) (4)	σ (km s^{-1}) (5)	N (6)
VY2–3....	Left	λ4861	−32	12	7
		λ4959	−44	12	7
		λ5007	−45	11	7
		λ6563	−50	10	4
		λ6563*	−45	8	6
	Right	λ4861	−24	9	6
		λ4959	−29	6	6
		λ5007	−42	7	6
		λ6563	−39	11	3
		λ6563*	−43	5	6
M1–2	Left	λ4861	0	8	4
		λ4959	−23	5	4
		λ5007	−16	5	4
		λ6563*	−9	6	4
	Right	λ4861	+7	10	4
		λ4959	−7	11	4
		λ5007	−18	7	4
		λ6563*	−2	3	4

* Observed during the 1974 observing season.

Table 4 shows that the standard deviation for a single line is typically 10 km s^{-1}, which is equal to our measuring errors. Since the observations span two observing seasons, this shows that the ITD and Lick Cassegrain spectrograph is a stable system. The small standard deviations show the suitability of the system for accurate radial-velocity observations of faint (~21 mag) emission-line objects.

There are small but apparently significant differences between the velocities from different lines and from the two slits. In M1–2, O'Dell (1966) found no measurable velocity difference between the lower members of the Balmer series and the forbidden lines. O'Dell used nine spectra of M1–2 to determine the emission-line velocity $v_0 = -17.6 \pm 2.5$ km s^{-1}. Our λ5007 velocities from the two slits ($\bar{v}_{\lambda 5007} = -17$ km s^{-1}) agree well with this value.

Perek and Kohoutek (1967) quote a private communication from Mayall which gives −55 km s^{-1} for the heliocentric velocity of VY2–3. An estimate of the uncertainty was not given. Our left and right slit velocities from λ5007 are in close agreement and give a mean velocity $v_0 = -43.5$ km s^{-1}. In view of the agreement between the ITS 5007 velocity of M1–2 and O'Dell's velocity, we adopt our velocity (−43.5 km s^{-1}) for the radial velocity of VY2–3.

Since the velocities from λ5007 constitute a consistent set of data, we derive correction factors for the other lines relative to λ5007. These correction factors are given in Table 5. The last column gives the total number of velocity measurements used to determine the correction factors. It should be emphasized that the corrections are small and that they will not enter in future determinations of velocity dispersion.

The standard deviation of a velocity determination does not depend strongly on the brightness of the

TABLE 5
CORRECTION FACTORS FOR ITS EMISSION-LINE RADIAL VELOCITIES

Slit	Line	Correction (km s^{-1})	Standard Error (km s^{-1})	N
Left......	λ4861	−14	5	22
	λ4959	+2*	2	22
	λ6563	−1*	5	25
Right.....	λ4861	−21	4	20
	λ4959	−13	3	20
	λ6563	−6	4	25

* No correction factor will be used.

nebula. The brightest planetary nebula in M32, NGC 221-1 (cf. Paper II), was observed on five separate nights in 1974. The velocities determined from the lines λλ6548, 6563, and 6584 gave a standard deviation of 10 km s^{-1}.

d) *Radial Velocities of Nebulae in NGC 185 and NGC 147*

The radial velocities of planetary nebulae in NGC 185 and NGC 147 are presented in Table 6. The first column gives the designations of the nebulae; the weighted mean velocity for the date of observation is immediately below the designation. Columns (2) through (5) give the date of the observation, the slit, the emission line, and the heliocentric velocity. The last column gives relative weights assigned during measurement on the basis of line symmetry and strength.

We adopt the weighted mean of the three sets of observations in Table 6 for the radial velocity of NGC 185. The mean, -208 ± 4 km s^{-1}, should be considerably more accurate than the value of −252 km s^{-1} determined by Humason, Mayall, and Sandage (1956).

During the 1976 observing season, the planetary nebulae NGC 185-1 and NGC 147-1 were observed on two nights with the Kitt Peak National Observatory image-intensifier–image-dissector scanner (IIDS) on the Mayall 4 m telescope. Except for the fact that the nebulae were observed in only one aperture, the observing procedure and reductions were as described by Ford and Jenner (1976). The data are given in Table 7. The column headings have the same meaning as in Table 6.

The average velocity of NGC 185-1 determined at Kitt Peak differs by only 10 km s^{-1} from the average velocity derived at Lick. Since the Lick velocities are tied to a system of radial-velocity standards, we choose to apply a small 10 km s^{-1} correction to Kitt Peak data to bring them to the Lick system. The correction has no effect on the velocity *difference* between NGC 185-1 and NGC 147-1. The differences determined on the two nights are −32 km s^{-1} and −37 km s^{-1}. When they are averaged with the Lick difference of −52 km s^{-1}, we obtain -40 km s^{-1} $\pm$ 6 km s^{-1} for the average difference between the radial velocities of NGC 185-1 and NGC 147-1. We adopt this value for the difference between the radial velocities of the two galaxies. The radial velocity of NGC 147 in the Lick system is then −168 km s^{-1}, with an estimated uncertainty of approximately 10 km s^{-1}.

IV. DISCUSSION

a) *Are NGC 185 and NGC 147 a Physical Pair?*

Baade (1944) estimated a distance of 204 kpc to NGC 185 and NGC 147. At this distance their projected separation (58′.2) corresponds to 3.5 kpc. Based on this implied close proximity, Baade concluded that the two galaxies "obviously form a physical pair." Modern estimates of the distance to NGC 185 and NGC 147 (~600 kpc, Hodge 1963) make Baade's conclusion less obvious. The radial velocities in this paper provide the basis for a quantitative discussion of the dynamical relationship of the two galaxies.

A *minimum* mass of $3.8 \times 10^9\ M_\odot$ is required to

TABLE 6
LICK RADIAL VELOCITIES OF PLANETARY NEBULAE IN NGC 185 AND NGC 147

Planetary Nebula V_0 (km s^{-1}) (1)	Date Observed (1975) (2)	Slit (3)	Line (4)	V_0 (km s^{-1}) (5)	Weight (6)
NGC 185-1.........	Sept. 6–7	Left	λ4959	−220	½
−215			λ5007	−202	1
		Right	λ4959	−208*	½
			λ5007	−229	1
NGC 185-1.........	Nov. 6–7	Left	λ4861	−194*	⅓
−208			λ4959	−211	½
			λ5007	−212	1
NGC 185-2.........	Nov. 6–7	Left	λ4861	−214*	1
−200			λ4959	−191	1
			λ5007	−195	1
NGC 147-1.........	Nov. 6–7	Left	λ4861	−160*	⅓
−157			λ4959	−160	½
			λ5007	−155	1

* A velocity correction was added to the observed velocity.

TABLE 7

KITT PEAK RADIAL VELOCITIES OF PLANETARY NEBULAE IN NGC 185 AND NGC 147

Planetary Nebula V_0 (km s^{-1}) (1)	Date Observed (1976) (2)	Slit (3)	Line (4)	V_0 (km s^{-1}) (5)	Weight (6)
NGC 185-1.........	Nov. 16–17	Left	λ4861	−224	½
−222.5			λ4959	−216	½
			λ5007	−225	1
NGC 185-1.........	Nov. 18–19	Left	λ4861	−214	½
−217			λ4959	−206	½
			λ5007	−224	1
NGC 147-1.........	Nov. 16–17	Left	λ4861	−207	½
−191			λ4959	−181	½
			λ5007	−187	1
NGC 147-1.........	Nov. 18–19	Left	λ4861	−147	½
−181			λ4959	−188	½
			λ5007	−195	1

gravitationally bind the pair with the observed 40 km s^{-1} radial-velocity difference and a projected separation of 10.5 kpc. The true mass will average 3.4 times the minimum mass for a large number of randomly oriented bound pairs selected to have the same projected separation. As we shall show, acceptance of even the minimum mass requires that NGC 185 and NGC 147 have a mass-to-light ratio (MLR) remarkably different from that of the well-studied elliptical galaxy M32.

The following values are adopted for the apparent integrated V-magnitudes of the galaxies:

m_V, NGC 147 = 10.46 (Hodge 1976);

m_V, NGC 185 = 9.4 (Hodge 1963); and

m_V, M32 = 8.31 (de Vaucouleurs 1975).

The visual absorption for the three galaxies is uncertain. McClure and Racine (1969) used reddening of late-type stars in the direction of M31 to derive a color excess $E(B - V) = 0.11 \pm 0.02$ for M31, a value which is approximately half that obtained from the cosecant law. Furthermore, van den Bergh (1976) has IIIa-J plates which suggest that this low absorption region extends to the lower galactic latitude region of NGC 147 and NGC 185. On the other hand, the Balmer decrement derived from our spectrophotometry of the brightest planetary nebula in NGC 185 implies that the color excess is approximately that predicted by the cosecant law. We further note that M32 may be behind M31, in which case it would be reddened by the disk of M31. In view of these considerations, we conservatively adopt the cosecant law $A_V = 0.26 \csc b$. If the color excess determined by McClure and Racine is correct, our use of the cosecant law will result in an overestimate of the luminosities and masses of NGC 147 and NGC 185 by approximately 40%.

We assume a distance of 600 kpc for NGC 185 and NGC 147, and 690 kpc for M32. The resultant absolute visual magnitudes are: M_V, NGC 147 = −14.47, M_V, NGC 185 = −15.53, and M_V, M32 = −16.59. Combining these values with the minimum binding mass $3.8 \times 10^9\ M_\odot$ and a provisional mass of $4.3 \times 10^8\ M_\odot$ for M32 (cf. § IV*b*) shows that binding requires the MLR of the pair to be *at least* 17 times larger than the MLR of M32. The small differences between the colors of the three galaxies (Sandage 1972) severely constrain any attempt to account for the large MLR by postulating differences between the luminosity functions of the pair and M32. The fact that the $B - V$ color of M32 is redder than those of NGC 185 and NGC 147 is in the wrong sense to account for a larger MLR in the pair by postulating a large number of faint red stars. If it is assumed that the two galaxies have halos of nonluminous matter, the halos must have a mass approximately 17 larger than the mass of the luminous stars. We consider this an unlikely possibility. Finally, we note that the assumption that the pair is bound and has the same MLR as M32 requires the observed velocity difference to be *less* than 9.7 km s^{-1}. This is incompatible with the observed difference of 40 km s^{-1} by approximately 3 σ. Thus, we conclude that NGC 185 and NGC 147 are not a gravitationally bound system.

b) The Interstellar Media and Galactic Winds

The five planetary nebulae identified in NGC 147 and the five identified in NGC 185 provide an observational basis for estimating the lower limit to the production rate of the interstellar medium in these galaxies. Unlike M32, the observed numbers in these low-surface-brightness galaxies require a negligible correction for nebulae lost against the central envelopes. In Paper II it was conservatively estimated that the ~2.5 mag difference between the brightest and faintest nebulae on our plates corresponds to 12,000 years of evolution. Assuming 0.2 $M_\odot$ per planetary shell, the production rate of the interstellar medium in these galaxies is at least $\dot{M} \geq 8.3 \times 10^{-5}\ M_\odot\ \mathrm{yr}^{-1}$. The major uncertainties in this estimate are due to the statistics of the small sample and the difficulty of assigning reliable evolutionary times to planetary nebulae.

In Paper II it was concluded that the present production rate of planetary nebulae is comparable with the production rate for the past 10^{10} years. The disposition of the resultant *minimum* of $10^6\ M_\odot$ in NGC 147 and NGC 185 is of considerable interest. Two of the four elliptical companions of M31—NGC 185 and NGC 205—have conspicuous dust clouds and OB stars (Baade 1944, 1951; Hodge 1963, 1973), whereas NGC 147 and M32 have no detectable interstellar media (cf. Paper II for a discussion of the interstellar medium in M32). Hodge (1963) has estimated $2 \times 10^5\ M_\odot$ for the mass of the OB stars in NGC 185. If disposal mechanisms such as a galactic wind are inoperable, the planetary nebulae alone will provide the necessary mass in less than 2.5×10^9 years.

In Paper II Ford and Jenner discussed the possibility that a supernova-heated wind (Mathews and Baker 1971) blows in M32. They noted that demonstrating thermal stability in a steady-state supernova-heated wind in a low-mass elliptical galaxy is not sufficient to show that a wind can be established in the first place. Depending on the dynamical structure of the galaxy, the ejected gas may be thermalized at temperatures where radiative cooling will proceed more rapidly than supernova heating, thereby preventing establishment of the wind. On the other hand, in a low-mass galaxy such as NGC 147, the planetary shells may be ejected at velocities sufficiently larger than the stellar velocity dispersion to thermalize the gas at a temperature which will give a wind without supernova heating.

We will first show that the mass and stellar concentration in NGC 147 are so low that the kinetic energy in the expanding planetary shells is sufficient to energize a wind. Though the shells will have expansion velocities in excess of the escape velocity (v escape ≈ 13 km s^{-1}) in a large fraction of the galaxy, the characteristic time to cross the galaxy ($\sim 2 \times 10^7$ years) is much longer than the mean time between formation of planetary nebulae ($\sim 2 \times 10^3$ years). Thus we expect planetary shells to collide within NGC 147. The radiative cooling time for colliding shells with radii larger than 3 pc is much longer than the time required for sound waves or shocks to cross the shells, whereas the relaxation time for protons in colliding shells is much shorter than the interaction time. Consequently, the colliding shells will interact with one another adiabatically and thermalize at a temperature of $\sim 10^4$ K.

To investigate the thermal stability of a wind, we use Mathews and Baker's linearization of the flow-governing equations. Those authors have shown that this first-order solution agrees well with the numerical solution of the nonlinear equations in giant ellipticals. The parameters required for a solution are the mass of the galaxy M, a characteristic length which we take to be the core radius r_c, a dimensionless mass μ (King 1966), a characteristic velocity dispersion v_s, and a mass loss rate $\dot{M}$. The masses for NGC 147 and NGC 185 were estimated from the ratio of their integrated magnitude to that of M32 and the assumption that they have the same mass-to-light ratio as M32. A preliminary reduction of the planetary radial velocities in M32 gives a halo velocity dispersion of 35 km s^{-1} and a virial mass of $4.3 \times 10^8\ M_\odot$. This is a substantial revision of the value $1.3 \times 10^9\ M_\odot$ determined by Richstone and Sargent (1972). Using their value of 60 km s^{-1} for the nuclear velocity dispersion, we determine a mass of $4 \times 10^8\ M_\odot$ from a King model. We adopt $4.3 \times 10^8\ M_\odot$ as a provisional mass for M32; the estimated masses for NGC 147 and NGC 185 were scaled from this value. The stellar velocity dispersions in NGC 147 and NGC 185 were scaled from the planetary velocity dispersion observed in M32. For the scaling we used the virial theorem and an estimate of the fraction of the mass of each galaxy which is interior to the mean reciprocal radius $2\pi^{-1}\langle 1/r\rangle$ of its planetary nebulae. The adopted parameters are tabulated in Table 8. We emphasize that many of the numbers in Table 8 are estimates rather than direct measurements.

The criterion for a thermally steady wind is that the cooling time in the center of the galaxy be much greater than the time required for the gas to flow a characteristic length. The core radius r_c is a natural characteristic length, since it is approximately an e-folding distance for the stellar density and consequently the gas density. The flow time is defined as the core radius divided by the sound speed at the center of the galaxy.

The linear solution with no supernova heating is given in Table 8. Successive rows give the temperature equivalent (T_s) of the quadratic sum of the stellar velocity dispersion and an assumed planetary shell expansion velocity of 20 km s^{-1}, the central temperature (T_c), the sound speed (c), particle density (n), cooling time ($t_{\rm cool}$) at the center of the galaxy, and the flow time ($t_{\rm flow}$). The 6000 K central temperature is based on the assumption that there is a minimum temperature set by heating from horizontal-branch stars (Mathews and Baker 1971).

The linear solution shows that a wind in NGC 147 is thermally steady even in the absence of supernova heating. This conclusion is relatively insensitive to the assumed mass loss rate; the mass loss rate must be

TABLE 8

GALAXY PARAMETERS

Parameter	NGC 147	NGC 185	M32
$M(M_\odot)$	6.1×10^7	1.6×10^8	4.3×10^8
$r_{\rm core}$(pc)	195	125	14
$r_{\rm tidal}$(pc)	1950	2909	1204
μ	11.8	19	45
$\pi/2\langle 1/r\rangle^{-1}$	567	295	446
$v_{\rm stellar}$(km s^{-1})	8	17	61
$\dot{M}(M_\odot\ {\rm yr}^{-1})$	8.3×10^{-5}	8.3×10^{-5}	5.7×10^{-4}

Linearized Cool Wind Solution in NGC 147

T_{sn}	0
T_s	9.4×10^3 K
T_c	6.0×10^3 K
c	1.3×10^6 cm s^{-1}
n	5.9×10^{-4} cm^{-2}
$t_{\rm cool}$	7.6×10^8 yr
$t_{\rm flow}$	4.4×10^7 yr

increased by more than a factor of 4 to quench the wind.

Since the interaction of the planetary shells results in a thermally stable interstellar medium, it appears likely that supernovae can heat the interstellar medium and cause a hot wind to blow. Though the linear solutions for a hot wind in NGC 147 are not self-consistent, in that they predict relaxation times which greatly exceed flow times, they do show that a supernova rate within an order of magnitude of one per 50 years per 10^{11} stars will heat the cool wind sufficiently for a hot ($T \approx 10^7$ to 10^8 K) wind to blow.

We conclude that a wind is blowing in NGC 147. The wind may be a thermally steady cool wind which is powered by expanding planetary shells, a thermally steady hot wind which is powered by supernovae, or a wind which blows hot and then cool. The present uncertainties in the frequency and energy release of Type I supernovae in elliptical galaxies prevent us from determining the precise nature of the wind.

The scenario of filling a galaxy with a thermally stable gas which can be heated by supernovae does not work in NGC 185 and M32. In the absence of supernovae, the gas will rapidly cool and accumulate in the center of the galaxy. In the presence of supernovae, the history of a planetary shell will be a statistical sequence of interactions with a distribution of sizes of planetary and supernovae shells. Determination of the fate of the shells will require an analysis of these interactions.

This work was supported in part by a grant from the Research Corporation and by grants from the UCLA Academic Senate Research Committee. Computing funds were provided by a grant from the UCLA Campus Computing Network. The image-intensifier instrumentation resulted from NSF grant 50-262-0102 to Dr. Russell J. Donnelly at the University of Oregon. The determination of coordinates in the AGK3 system was made possible by two astrograph plates kindly taken for us by Dr. Arnold Klemola. We are grateful to Dr. Donald E. Osterbrock for permission to use plates from the Lick Observatory plate file and to Dr. Sidney van den Bergh for a critical reading of the manuscript.

We wish to thank Dr. Leo Goldberg and the Kitt Peak Time Assignment Committee for the allocation of time on the Mayall 4 m telescope. The Kitt Peak staff provided excellent assistance in the operation of the IIDS.

APPENDIX

GLOBULAR CLUSTERS IN NGC 185 AND NGC 147

I. NGC 185

Baade (1944) identified two globular clusters in NGC 185. These clusters, which are numbers III and V in Figure 2, are described by Baade as being similar in structure and diameter to the clusters in the Andromeda Galaxy (M31).

We systematically searched Mayall's plate of NGC 185 (cf. § II*b* and Fig. 2) for additional globular clusters. The plate is excellent for this purpose, since it has a large field (28′.7 × 40′.1) and resolves the galaxy into stars. On the plate envelope Mayall noted the presence of six possible globular clusters; regrettably, these were no longer marked on the back of the plate.

The plate was searched for objects which appeared to be nonstellar, circular, and partially resolved into stars. Using these criteria, we found four probable globular clusters and two possible globular clusters in addition to Baade's two clusters. The probable globular clusters are identified by roman numerals I through VI in Figure 2. Of these, only cluster V is clearly resolved into stars. The remaining five clusters show a granularity (partial resolution) which can be distinguished from the smooth density gradients in the background elliptical galaxies. Though object VII is nonstellar and circular, it is too faint to judge the resolution; consequently, we can only note that it may be a faint globular cluster. Object VIII would be considered a probable globular cluster except for the fact that it projects onto a faint cluster of galaxies. Parentheses are placed around objects VII and VIII in Figure 2 to emphasize that they could be galaxies.

Hodge (1974) identified globular clusters in NGC 185 from a V plate taken with the Lick Observatory 120 inch telescope and from the collection of Baade's plates at the Hale Observatories taken with the 100 inch (2.5 m) and the 200 inch (5 m) telescopes. The difficulty of distinguishing between faint background galaxies and globular clusters is apparent from the fact that there are only four objects in common between Hodge's and our identifications. Hodge's (1974) photoelectric colors show that these objects, I (Hodge 1), II (Hodge 3), III (Hodge 4), and V (Hodge 5) are almost certainly globular clusters. The nature of our objects IV, VI, VII, and VIII, which Hodge rejected, and Hodge 2, which we rejected, is less certain. *B*, *V* or *U*, *B*, *V* photoelectric observations will be the most efficient means of determining whether the objects are faint galaxies or globular clusters.

Three plates were used to determine the positions of the clusters: Mayall's direct plate ED 354, and the two image-intensifier plates ED 2575 and ED 2586 (cf. § II*b*). The *x* and *y* positions of the clusters on the image-intensifier plates were transformed to equatorial coordinates along with those of the planetary nebulae. Mayall's plate was reduced in exactly the same way as the image-intensifier plates.

The coordinates determined from the three plates were averaged and the deviations from the means were computed. Plate ED 2575 had the largest deviations

TABLE 9

COORDINATES OF GLOBULAR CLUSTERS IN NGC 185 AND NGC 147

Cluster	Right Ascension (1975.0)	Declination (1975.0)
	NGC 185	
I..........	00h37m19s75	48°10′27″1
II..........	00 37 25.15	48 10 02.9
III..........	00 37 40.72	48 11 44.2
IV..........	00 37 49.18	48 14 35.3
V..........	00 37 50.37	48 14 51.9
VI..........	00 37 51.84	48 12 01.6
VII*.......	00 37 55.28	48 14 50.8
VIII*†......	00 38 00.65	48 10 32.3
	NGC 147	
I..........	00 31 49.94	48 22 16.4
II..........	00 31 52.92	48 19 07.3
III..........	00 31 51.34	48 20 32.6
IV‡........	...	...

* Possibly a galaxy rather than a globular cluster.

† The coordinates were determined from only one plate, ED 352.

‡ Too faint for a precise location with our plate material.

from the means, reflecting the fact that this plate was taken during poorer seeing than the other two plates. Consequently, the coordinates from ED 2575 were given one-half weight relative to the coordinates from the other two plates.

The weighted average coordinates are presented in Table 9. The column headings have the same meaning as in Tables 2 and 3. The average standard deviation from the mean coordinate is 0″3 in right ascension and declination. The coordinates should have a precision of at least 1″ relative to the AGK3 and at least 0″5 relative to the reference stars in Table 3.

II. NGC 147

Baade (1944) identified a semistellar nucleus and two globular clusters in NGC 147 (clusters II and III in Fig. 1). We used two plates to search for additional clusters: the Hα interference filter photograph ED 2670 (see § II*a* and Fig. 1) and a 120 inch telescope direct plate, ED 352. The latter was a 40-minute exposure by Mayall using a 103a-E plate, a GG 11 filter, and the B Ross corrector. Because of mediocre seeing, the plate did not resolve NGC 147 into stars. On the plate envelope Mayall noted the presence of two possible globular clusters.

No additional clusters were found. However, the fact that the "nucleus" (object I in Fig. 1) appeared to be slightly displaced from the center of the light distribution led us to conclude that it is more likely a globular cluster than the nucleus of the galaxy. Hodge (1976) reached the same conclusion on the basis of quantitative data. He found that the "nucleus" is displaced by 15″ from the center of the elliptical isophotes and has a photoelectric color which, when compared to the color of the galaxy, suggests that it is a globular cluster.

Hodge (1976) found that cluster I and Baade's two clusters are resolved into stars on the best 200 inch Hale telescope plates. Furthermore, he was able to identify a faint fourth cluster. The Lick plate material is not deep enough to allow a precise location of the cluster; the approximate position is indicated by roman numeral IV in Figure 1.

The equatorial coordinates of the three brightest clusters were determined from identical reductions of the plates ED 352 and ED 2670. The reduction of the latter is described in § II*a*. The averages from the two plates are presented in Table 9. The average difference between the two sets of coordinates is 0″1 in right ascension and 0″3 in declination. The coordinates have the precision typical for our reduction procedure.

REFERENCES

Arp, H. A. 1964, *Ap. J.*, **139**, 1378.
Baade, W. 1944, *Ap. J.*, **100**, 147.
———. 1951, *Publications of the University of Michigan*, **10**, 7.
Bowen, I. S. 1960, *Ap. J.*, **132**, 1.
Broadfoot, A. L., and Kendall, K. R. 1968, *J. Geophys. Res.*, **73**, 426.
de Vaucouleurs, G. 1975, private communication.
Eichhorn, H. 1974, *Astronomy of Star Positions* (New York: Ungar).
Ford, H. C., and Jenner, D. C. 1975, *Ap. J.*, **202**, 365 (Paper II).
———. 1976, *Ap. J.*, **208**, 683 (Paper III).
Ford, H. C., Jenner, D. C., and Epps, H. W. 1973, *Ap. J. (Letters)*, **183**, L73 (Paper I).
Hodge, P. W. 1963, *A.J.*, **68**, 691.
———. 1973, *Ap. J.*, **182**, 671.
———. 1974, *Pub. A.S.P.*, **86**, 289.
———. 1976, *A.J.*, **81**, 25.
Humason, M. L., Mayall, N. U., and Sandage, A. R. 1956, *A.J.*, **61**, 97.
King, I. R. 1966, *A.J.*, **71**, 64.
Mathews, W. G., and Baker, J. C. 1971, *Ap. J.*, **170**, 241.
McClure, R. D., and Racine, R. 1969, *A.J.*, **74**, 1000.
Miller, J. S., Robinson, L. B., and Wampler, E. J. 1975, *Advances in Electronics and Electron Physics* (New York: Academic Press).
O'Dell, C. R. 1966, *Ap. J.*, **145**, 487.
Perek, L. and Kohoutek, L. 1967, *Catalogue of Galactic Planetary Nebulae* (Prague: Academia).
Richstone, D., and Sargent, W. L. W. 1972, *Ap. J.*, **176**, 91.
Robinson, L. B., and Wampler, E. J. 1972*a*, *Pub. A.S.P.*, **84**, 161.
———. 1972*b*, *Ap. J. (Letters)*, **171**, L83.
Sandage, A. 1972, *Ap. J.*, **176**, 21.
van den Bergh, S. 1976, private communication.

HOLLAND C. FORD, GEORGE JACOBY, and DAVID C. JENNER: Department of Astronomy, University of California, Los Angeles, CA 90024

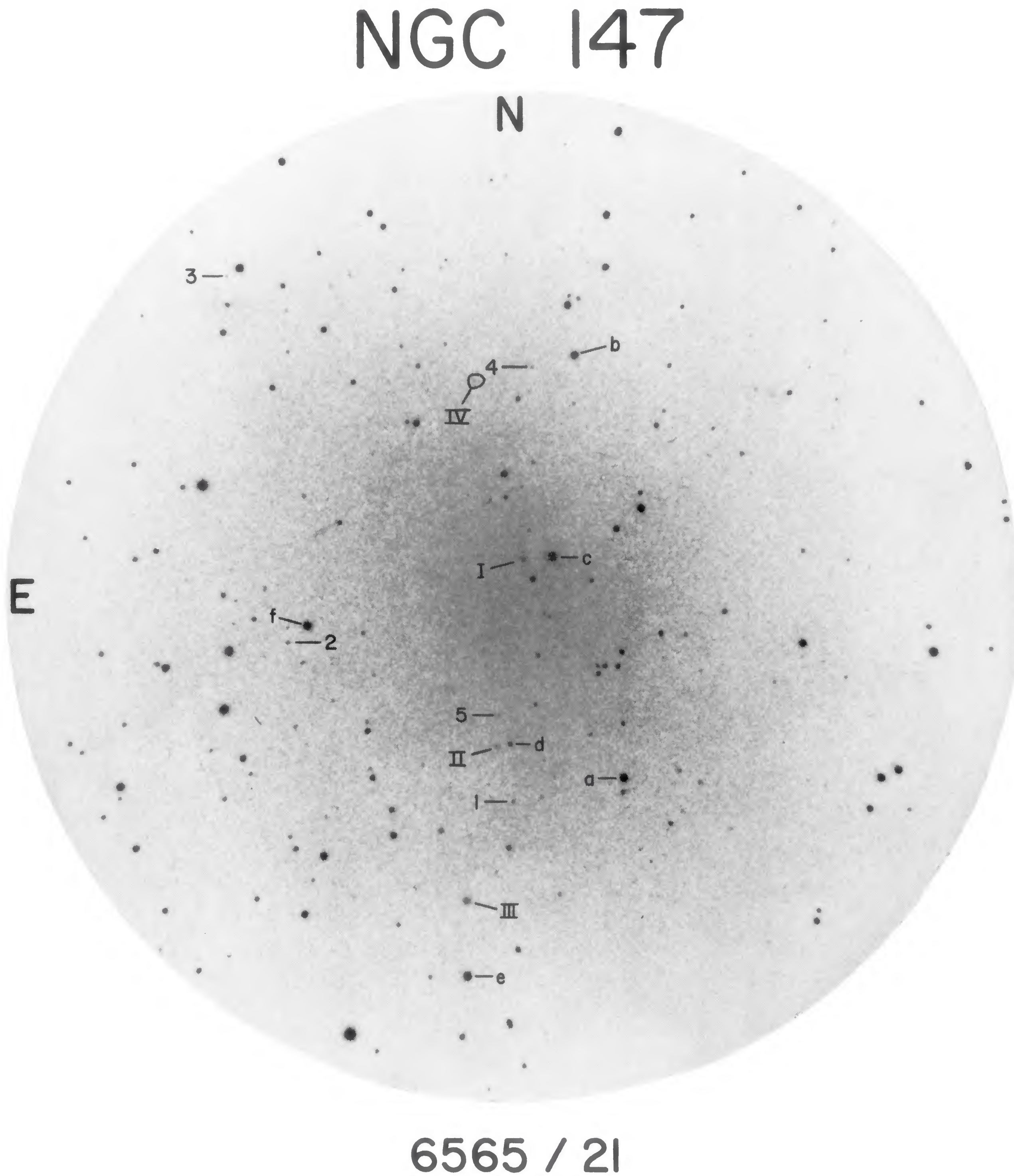

FIG. 1.—Identifications of five planetary nebulae and four globular clusters in NGC 147. The image-intensifier plate (IIa-D) isolates Hα with the interference filter λ_c6565 (21 Å FWHM). Planetary nebulae are labeled with arabic numbers, globular clusters are labeled with roman numerals; the reference stars are labeled with roman letters. Coordinates are presented in Table 2 and Table 9. The field is 9'.4 in diameter.

FORD *et al.* (*see* page 18)

NGC 185

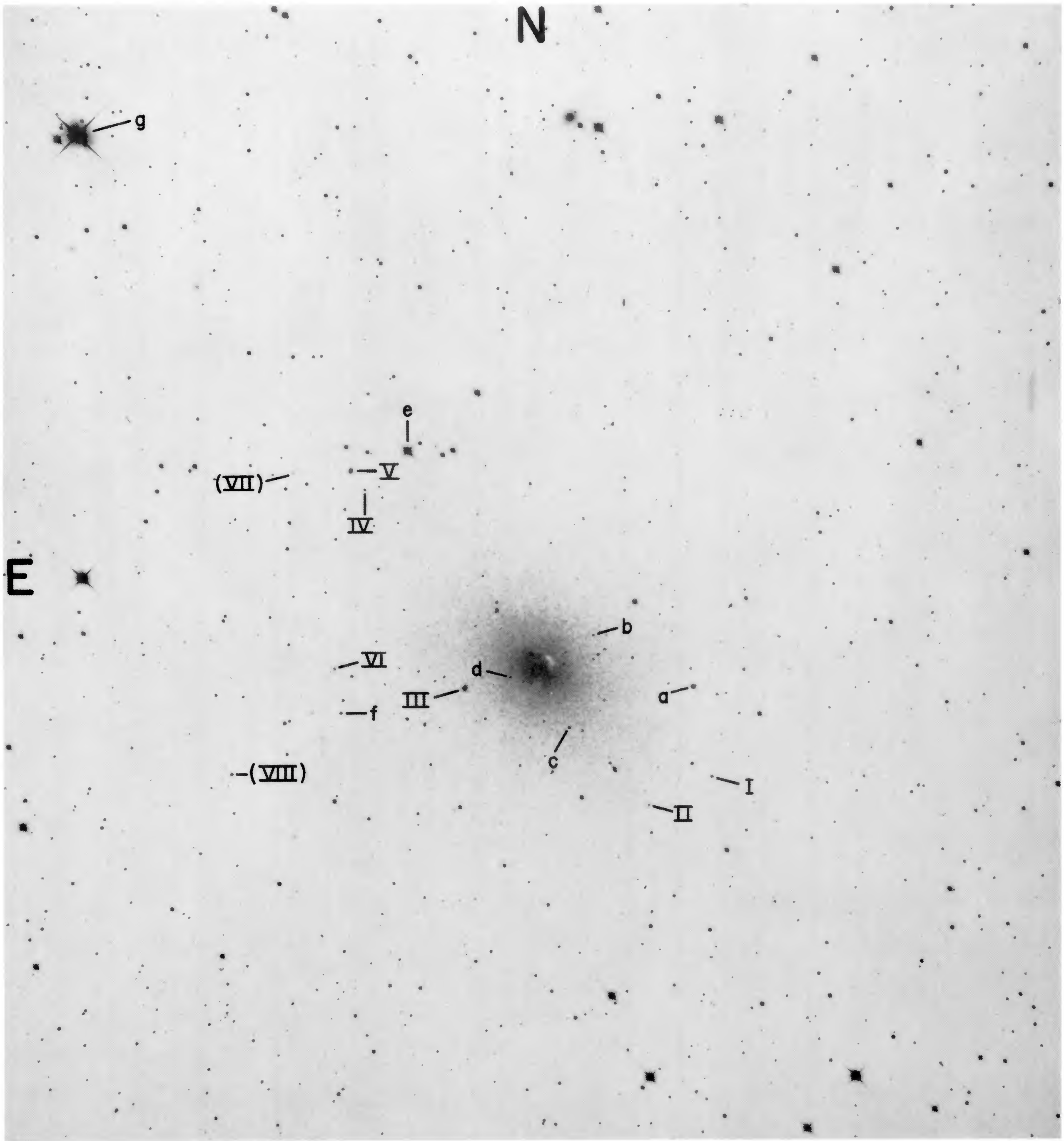

FIG. 2.—Identifications of six probable and two possible globular clusters in NGC 185. The 40-minute exposure by Dr. N. U. Mayall with a 103a-E plate and Schott GG 11 filter at the prime focus of the Lick Observatory 120 inch telescope resolves NGC 185 into stars. The probable globular clusters are labeled with roman numerals; parentheses indicate two possible clusters. Reference stars are labeled with roman letters. Coordinates for the globular clusters and reference stars are given in Table 9 and Table 3. The field size is 15′.0 × 16′.1.

FORD *et al.* (*see* page 19)